An XPS analysis of the interaction of *meso*-tetrakis(*N*-methylpyridinium-4-yl)porphyrin with exfoliated manganese thiophosphate

2006 J. Phys.: Condens. Matter 18 5759

(http://iopscience.iop.org/0953-8984/18/24/016)

INSTITUTE OF PHYSICS PUBLISHING JOURNAL OF PHYSICS: CONDENSED MATTER

J. Phys.: Condens. Matter **18** (2006) 5759–5772 doi:10.1088/0953-8984/18/24/016

An XPS analysis of the interaction of *meso*-tetrakis(*N*-methylpyridinium-4-yl)porphyrin with exfoliated manganese thiophosphate

L Silipigni[1,2,5], G De Luca[3], T Quattrone[2], L Monsù Scolaro[3], G Salvato[4] and V Grasso[1,2]

[1] Dipartimento di Fisica della Materia e Tecnologie Fisiche Avanzate, Università di Messina, Salita Sperone 31, I, 98166 Messina, Italy
[2] Centro Siciliano per le Ricerche Atmosferiche e di Fisica dell'Ambiente, Salita Sperone 31, I, 98166 Messina, Italy
[3] Dipartimento di Chimica Inorganica, Chimica Analitica e Chimica Fisica and CIRCMSB, Università di Messina, Salita Sperone 31, I, 98166 Messina, Italy
[4] Istituto per i Processi Chimico-Fisici del CNR, sezione Messina, Via La Farina 237, I, 98123 Messina, Italy

E-mail: lsilipigni@unime.it

Received 24 October 2005, in final form 7 April 2006
Published 2 June 2006
Online at stacks.iop.org/JPhysCM/18/5759

Abstract

Composite thin films of $(C_{72}H_{66}N_8O_{12}S_4)_yLi_{2x}Mn_{1-x}PS_3$ have been obtained through a solution approach by interacting the tosylate salt of the cationic water soluble 5,10,15,20-tetrakis(*N*-methylpyridinium-4-yl)porphyrin (H_2T_4) and $MnPS_3$ exfoliated in the presence of lithium ions. The thin films have been investigated through x-ray diffraction (XRD), ultraviolet/visible (UV/vis) absorption and mainly x-ray photoemission spectroscopy (XPS). N 1s core-level XPS spectra emphasize the presence of three non-equivalent nitrogen atoms, similarly to the film of the pure H_2T_4 salt. This result, together with the interlayer spacing determined by the XRD pattern and the evidence from absorption measurements, indicates that the porphyrin is intercalated into $MnPS_3$ layers in a non-protonated form and substantially flattened with respect to the free molecule. The striking likeness between the N 1s core levels in the XPS spectra of the composite material, of the H_2T_4 salt and of the neutral meso-tetrapyridylporphyrin (H_2TP_yP) suggests that H_2T_4 is present between the $MnPS_3$ nanosheets together with its counter-ion (tosylate). This hypothesis is confirmed by the observation of a structure which can be attributed to the sulfur of the counterion in the S 2p core-level XPS spectra of the composite material. An analysis of the Mn 2p and 3p, S and P 2p core-level regions through XPS reveals a strong similarity between the starting $MnPS_3$ and the composite material, suggesting that no charge transfer occurs from the guest (H_2T_4-tosylate) to the host species ($MnPS_3$).

[5] Author to whom any correspondence should be addressed.

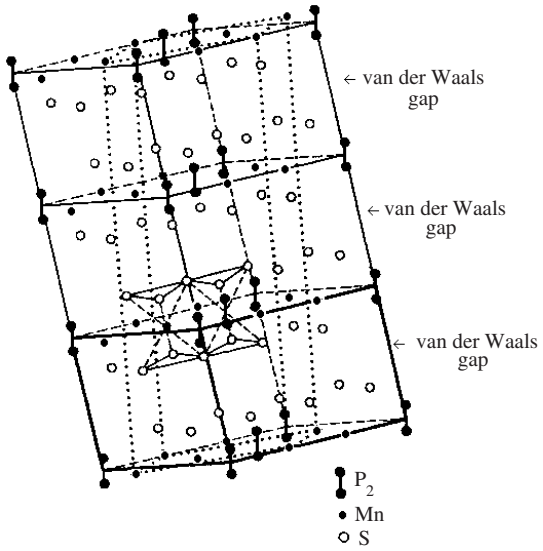

Figure 1. The $MnPS_3$ crystallographic cell [71].

1. Introduction

The research on advanced materials with potential technological application, especially in optoelectronics and photonics, is a very active area of interest. In this context, the intercalation of organic molecules into low-dimensional inorganic matrixes appears as a simple and useful technique for obtaining new hybrid organic–inorganic nanocompounds with interesting physico-chemical properties. These nanocomposites can be exploited in nonlinear optics, sensors, ionic conductors, molecular sieves, and so on.

Among the layered inorganic host matrixes, manganese thiophosphate ($MnPS_3$) exhibits, together with other transition metal thiophosphates [1, 2], a unique ion-exchange property, and consequently it is well suited to the synthesis of inorganic–organic composite materials at the molecular level [3–9]. The $MnPS_3$ structure is based on double layers of sulfur atoms interconnected by phosphorous and manganese atoms. These $[SMn_{2/3}(P_2)_{1/3}S]$ sandwiches, in which manganese is present as a bivalent cation, are stacked along the *c* axis and are held together by van der Waals forces, forming the so-called van der Waals interlayer gaps, which are normally empty (see figure 1).

As a result of the weak interlayer interactions, both neutral and charged guest molecules can be inserted into $MnPS_3$ van der Waals gaps through a variety of methods, leading to intercalated complexes. These latter species consist of alternating host ($MnPS_3$) and guest (G) layers, exhibiting different stoichiometry depending on the charge of the guest [1]. The method is very versatile, since pre-intercalated species may again be exchanged with other guests. When G is an alkali metal ion, negatively charged ($Mn_{1-x}PS_3$) layers are formed, owing to intercalation, and the presence of these hydrated cations makes the layers electrically neutral, as in the case of $CdPS_3$ [10]. $MnPS_3$ can be also exfoliated to single layers when it is first intercalated with potassium and then with lithium ions [11]; this behaviour being particularly interesting for obtaining orientated thin films.

In this framework, natural and synthetic porphyrins and metal porphyrin complexes can be regarded as interesting guest compounds, because they have been investigated extensively,

both in solid and solution phases, for their biological implications and technological applications [12, 13]. In particular, the insertion of porphyrins and metalloporphyrins into ordered matrixes is a topic of current interest because of their binding ability towards many species (e.g. dioxygen, carbon monoxide and nitric oxides) [14, 15] and their catalytic activity, as well as their photoactive and conductive properties [16]. Taking advantage of these specific properties, it is possible to obtain new functional materials for exploitation as photoconductors, optical actuators, and chemical or optical sensors. Porphyrins are also good photosensitizers, because of their favourable absorption spectra, which exhibit a strong B-band (Soret band, $\varepsilon \approx 10^5$–10^6 M^{-1} cm^{-1}) around 400 nm and a set of less intense Q-bands in the 500–700 nm region ($\varepsilon \approx 10^4$ M^{-1} cm^{-1}) [13]. In particular, water-soluble charged porphyrins are well suited to investigating electrostatic interactions and aggregation processes with matrixes bearing opposite charges in solution [17–28], since this process can be controlled conveniently by changing the medium properties, i.e. ionic strength and pH [29–35]. Furthermore, porphyrins can coordinate a large variety of metal ions in the central macrocycle, leading to the possibility of accessing the rich chemical properties of these derivatives (e.g. spectroscopic and redox properties, electron density, axial coordination).

Many porphyrins have been intercalated into inorganic layered materials such as smectite clays minerals [36], zirconium hydrogen phosphate [16], niobate [37], titanate [38] and layered double hydroxide [39], obtaining nanostructured materials that have been explored for photo-processes and catalytic reactions in confined media [40, 41]. In the case of porphyrins adsorbed on clays, the interaction improves the chemical stability, preventing a rapid photo-degradation of the organic macrocycles [42].

Despite the presence of this large body of literature, the interaction of porphyrins with $MnPS_3$ has not yet been reported. In the present study, we will focus on meso-tetrakis(*N*-methylpyridinium-4-yl)porphyrin (H_2T_4 hereafter), which is a water-soluble cationic synthetic porphyrin whose molecular structure is shown in scheme 1 together with its tosylate counterion. This molecule has largely been investigated for its ability to interact with nucleic acids through a variety of binding modes (mainly intercalation) [43], acting as a spectroscopic probe for local conformations. Due to the specific interaction with tumor cells, H_2T_4 has also been exploited in photodynamic therapy (PDT) for cancer treatment [44].

Thin films resulting from the interaction of H_2T_4 with exfoliated $MnPS_3$ have been investigated through x-ray diffraction (XRD), absorption measurements, and mainly x-ray photoemission spectroscopy (XPS) in order to get information about the chemical environment of involved species. We anticipate that H_2T_4 is intercalated into $MnPS_3$ together with its tosylate counterion as a neutral molecule, and a flattening of the meso substituent groups should be responsible for the observed optical properties. The presence of the guest seems not to alter the electronic properties of the host inorganic compound.

2. Experimental section

2.1. Preparation of the starting inorganic materials and interaction with H_2T_4

The preparation of the inorganic host material is a three-step process, essentially similar to that reported by Lagadic *et al* [11].

2.1.1. Synthesis of pure $MnPS_3$. $MnPS_3$ powders were prepared by heating a stoichiometric mixture of the elements of high purity at 750 °C for a week in sealed evacuated quartz tubes. The formation of $MnPS_3$ was confirmed by powder x-ray diffraction.

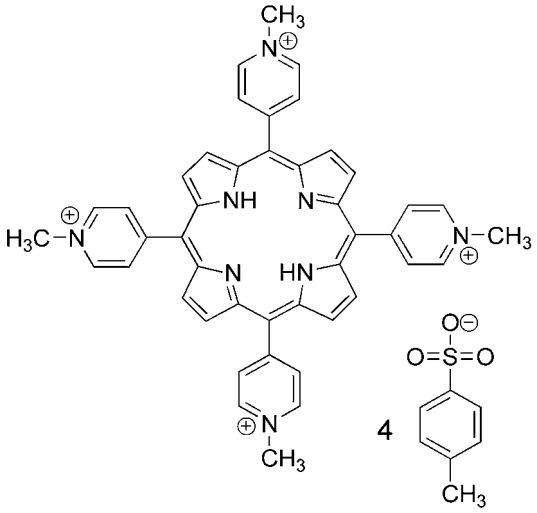

Scheme 1. Formula of the H_2T_4 tosylate salt.

2.1.2. Potassium ion intercalation ($K_{2x}Mn_{1-x}PS_3$). Polycrystalline powdered $MnPS_3$ samples (1 g) were first soaked in 2 M KCl aqueous solution (50 ml) and stirred at room temperature for 1 h to yield the intercalation compound $K_{2x}Mn_{1-x}PS_3$. The compound was sequentially washed several times with distilled water and de-ionized water and finally dried in an oven at 60 °C for 3 h. The ion-exchange reaction, which is unique to some MPS_3 [1], affords cationic vacancies in the layers and causes a dilation of the lattice [45]. Indeed, the completion of the ion-exchange intercalation process was ascertained by XRD measurements, checking that the original host (00*l*) peaks (spacing: 6.5 Å) have disappeared completely and that new (00*l*) peaks corresponding to a lattice spacing of 9.4 Å have appeared, in good agreement with the literature [8, 46].

2.1.3. Potassium for lithium ion exchange ($Li_{2x}Mn_{1-x}PS_3$). The potassium intercalated $MnPS_3$ powder was treated with a concentrated LiCl aqueous solution (3 M). The suspension that was obtained was stirred for 1 h at room temperature and allowed to settle for 30 min. The LiCl solution was renewed and the procedure was repeated once. Subsequently, the pale green precipitate was washed using LiCl aqueous solutions of decreasing concentration (0.5, 0.25 and 0.1 M) and washed three times with HPLC water, waiting about 15 min after each step. After this stage, the powder was highly dispersed in a pale green colloidal suspension.

2.1.4. Interaction of $Li_{2x}Mn_{1-x}PS_3$ with H_2T_4. H_2T_4 porphyrin was purchased from Aldrich Chem. Co. as tosylate salt ($C_{72}H_{66}N_8O_{12}S_4$; see also scheme 1) and used as received. An aqueous stock solution of this porphyrin was prepared and its concentration was determined to be 630 μM by UV–vis absorption measurements ($\varepsilon_{421} = 2.26 \times 10^5$ M^{-1} cm^{-1}) [47]. The previously obtained colloidal suspension was slowly added to 2 ml of the porphyrin solution while stirring at room temperature, until the colour of the solution turned from dark red to light yellow, indicating that only a small amount of porphyrin remained in solution. The brown precipitate was then collected and washed three times with doubly distilled water. This became stable under prolonged washing and/or hot digestion.

2.2. Thin film preparation

A few drops of the aqueous suspension of the nanocomposite material and of the starting lithium intercalate, as well as the stock porphyrin solution, were cast onto both glass slides and XPS sample holders and allowed to dry in dust-free air for at least two days.

2.3. XRD and XPS spectra on thin films

X-ray diffraction patterns were recorded in the $5° < 2\theta < 60°$ range with a Philips Analytics diffractometer model PW3710 using Cu Kα radiation (1.540 56 Å). The samples were examined as thin films deposited onto glass slides.

X-ray photoemission spectra were measured at room temperature using a VG Scientific photoelectron spectrometer equipped with an unmonochromatized conventional twin-anode Mg/Al Kα x-ray source, a 150° concentric hemispherical analyser (CLAM 100) operating in the constant pass-energy (CAE) mode at 20 eV, and a channeltron, whose voltage was fixed at 2.4 kV. The samples were examined as thin films, obtaining good electrical contact with the spectrometer. In the case of pure $MnPS_3$, the compound was analysed as pressed powder pellets. The Mg Kα line ($h\nu = 1253.6$ eV) was used as an excitation source. During each measurement, the analysis chamber pressure was in the 10^{-9} Torr range. No irradiation effects were detected on the investigated samples during the time needed to collect XPS spectra, indicating their stability to x-ray irradiation. The carbon C 1s line at 285.0 eV was used as a reference for the determination of the core-level peak binding energies. A least-square fitting procedure has been carried out on all the spectra, which have been fitted to Gaussian–Lorentzian cross-product profiles after having a Shirley-type inelastic background removed. The resulting best fit is shown in figures 3, 4 and 6 by a solid line, while the dashed lines are the component bands and the open circles are the experimental data.

2.4. Absorption measurements on nanocomposite and porphyrin thin films

Absorption measurements were carried out at room temperature on thin films of nanocomposite and H_2T_4 salt using a Perkin-Elmer double-beam UV–vis spectrophotometer (model Lambda 2). Unpolarized light struck the film surface at normal incidence. The analysed films were deposited on glass slides.

3. Results and discussion

The inorganic layered $MnPS_3$ compound can be exfoliated after the consecutive intercalation of potassium and lithium ions, respectively, according to a procedure reported by Lagadic *et al* [11]. The treatment of the compound with lithium chloride leads to an aqueous suspension containing nanosheets of the host material. This colloidal suspension is unstable, and after one day a pale green precipitate is obtained. The interaction of freshly prepared suspensions with the cationic H_2T_4 porphyrin in aqueous solution can be monitored easily through UV/vis spectroscopy by following the marked hypochromicity and bathochromic shift of the Soret band from 424 to 470 nm (figure 2). A titration of a porphyrin solution (3 μM) with exfoliated $Li_{2x}Mn_{1-x}PS_3$ leads to the progressive formation of an adduct, leaving only a tiny amount of free guest in solution. The arrows in figure 2 show a gradual decrease in intensity of the Soret band of the porphyrin in solution and the parallel appearance of the new feature due to the interaction of H_2T_4 with the inorganic matrix upon the addition of increasing amounts of exfoliated $Li_{2x}Mn_{1-x}PS_3$.

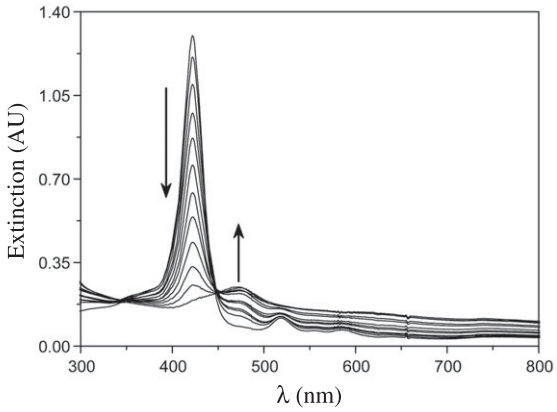

Figure 2. UV/vis spectral changes observed upon addition of increasing amounts of exfoliated $Li_{2x}Mn_{1-x}PS_3$ to a solution of H_2T_4 (3 μM).

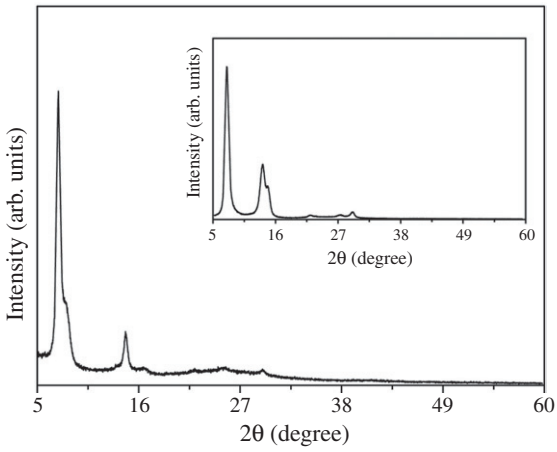

Figure 3. Powder XRD pattern for the nanocomposite and $Li_{2x}Mn_{1-x}PS_3$ (inset) thin films.

3.1. XRD analysis

Figure 3 reports the XRD spectrum of the composite material, whose pattern exhibits only 00*l* reflections, and whose peak position allows us to calculate a basal spacing of 12.1 Å. For the sake of comparison, the XRD spectrum of the precursor $Li_{2x}Mn_{1-x}PS_3$ thin film is shown in the inset, evidencing 00*l* reflections which give a basal spacing of 11.9 Å, in good agreement with the literature [11, 48]. On considering that the dimensions of H_2T_4 porphyrin are 17.5 Å × 17.5 Å × 4 Å [49], the observed small increase in the inter-lamellar distance on going from $Li_{2x}Mn_{1-x}PS_3$ to the porphyrin nanocomposite film rules out the occurrence of large structural changes in the stacking of the respective layers. Simple geometrical considerations suggest that the porphyrin plane cannot be perpendicular with respect to the $MnPS_3$ layers. Moreover, as already reported for $Li_{2x}Mn_{1-x}PS_3$ thin films [11, 48], even in the present compound the presence of only 00*l* reflections indicates a preferential orientation of the thin film, with the sheets stacking in a parallel fashion with respect to the glass substrate.

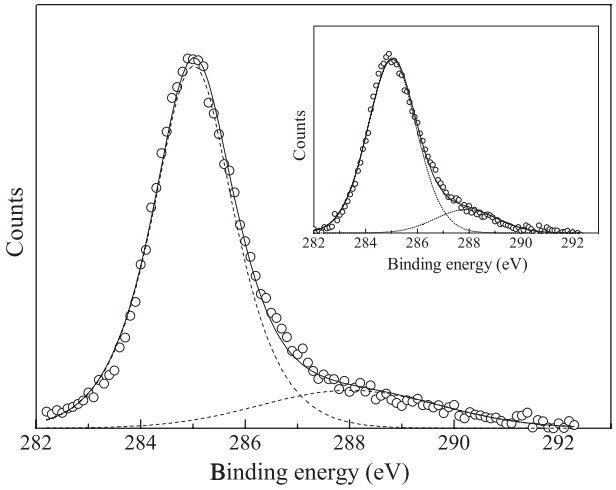

Figure 4. C 1s core-level XPS spectrum for the thin films of nanocomposite and H_2T_4 salt (inset). The solid line is the resulting best fit, while the dashed lines are the Gaussian–Lorentzian component bands.

3.2. XPS spectra

X-ray photoelectron spectroscopy (XPS) is a valuable tool in material sciences. Since the binding energies of the occupied core-electron levels depend on the local charge surroundings, the XPS peaks are good reporters of alteration in the chemical environment. In fact, in many cases a simple linear correlation exists between the partial ionic charge or oxidation state of an atom and the XPS chemical shift in a series of its compounds [72]. Thus it is possible to detect chemically non-equivalent atoms of the same element, differing in formal oxidation state or in molecular environment or in lattice site, and so on [50]. However, other factors, such as the atomic and extra-atomic relaxation of surrounding electrons towards the photoionized atom, can also contribute to the observed energy shifts, and they can even reverse the trend of the chemical shift from that predicted according to atomic charge. These final-state effects are significantly larger in the Auger process, since it involves two holes rather than one, as in the photoelectron process [72]. The interpretation of chemical shifts is complicated by the tendency for cations in transition metal compounds to show satellite features in the vicinity of the XPS core lines. However, the relative separation between the XPS main line and satellite (locally and non-locally screened XPS final states) should be sensitive to variations in the local cation charge environment. Therefore, chemical changes can be monitored by measuring the relative separations between the main line and satellite: the greater the local positive charge at the cation site, the greater is the expected satellite separation [73]. Nevertheless, the simple interpretation of binding energy shifts based on initial state concepts is extremely useful, especially for molecular solids [50], and valuable work can be performed by using the chemical shifts observed and tabulated in known systems as a fingerprint [74, 75]. On the basis of these considerations, in the present case the XPS technique can give insight into the potential occurrence of charge transfer processes between guest species and the host lattice.

Figures 4–7 report the C 1s, N 1s, S 2p, Mn 2p, P 2p, Mn 3p and Li 1s core region XPS spectra for the nanocomposite thin films. The fitting-deduced binding energy values are collected in table 1, where these values are compared with those measured for the parent $MnPS_3$ compound. In table 2, we report the atomic ratios derived from the XPS peak area

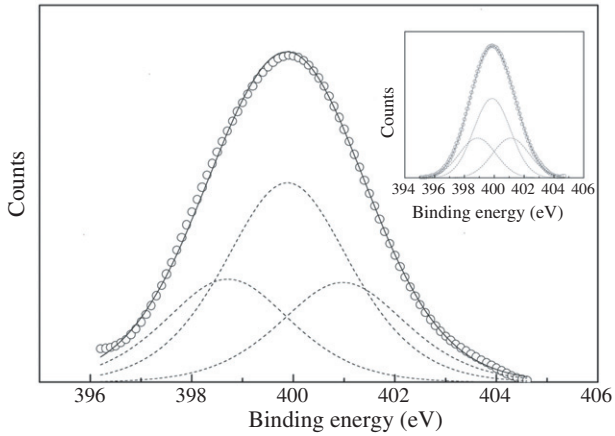

Figure 5. N 1s core-level XPS spectrum in the thin films of nanocomposite and H_2T_4 salt (inset).

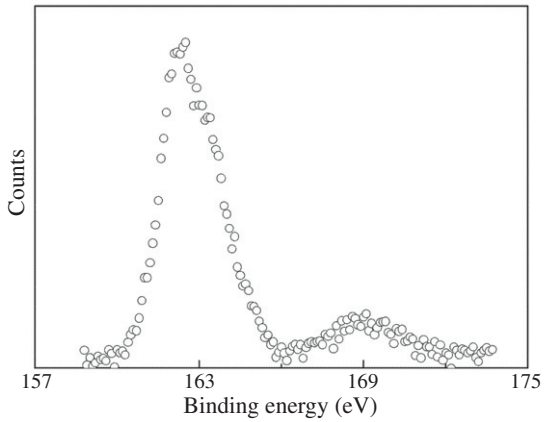

Figure 6. S 2p core-level XPS spectrum in the nanocomposite thin film.

using the tabulated relative atomic sensitivity factor for each constituent in the investigated sample (nanocomposite and H_2T_4 salt films) [76]. In this way, approximate values of 0.065 and 0.25 have been deduced for y and x, respectively, in the $(C_{72}H_{66}N_8O_{12}S_4)_yLi_{2x}Mn_{1-x}PS_3$ nanocomposite film, evidencing that the intercalated porphyrin salt is quite a small amount with respect to the hosting inorganic matrix.

The C 1s core-level XPS spectrum in these thin films consists of an asymmetric peak with a tailing on the higher-energy side, which underlies a weak structure (figure 4). The full width half maximum (FWHM) of the peak centred at about 285.0 eV is 1.8 eV. This value is larger than expected for a single type of carbon atom (FWHM = 1.06 eV), analogously to what has already been reported in the literature for tetraphenylporphyrin (H_2TPP) free base [51]. This observation suggests that the C 1s peak in the hybrid thin films is composite, deriving from the different carbon atoms present in H_2T_4, which are not detected as separate peaks because of their small difference in the 1s binding energy.

The weak feature at about 288.0 eV, shifted by ∼3.0 eV higher in binding energy with respect to the parent photo-peak, can be attributed to a shake-up satellite, as reported for H_2TPP and its copper complexes [51]. A similar spectrum is also obtained for the thin films of H_2T_4 salt, as shown in the inset of this figure.

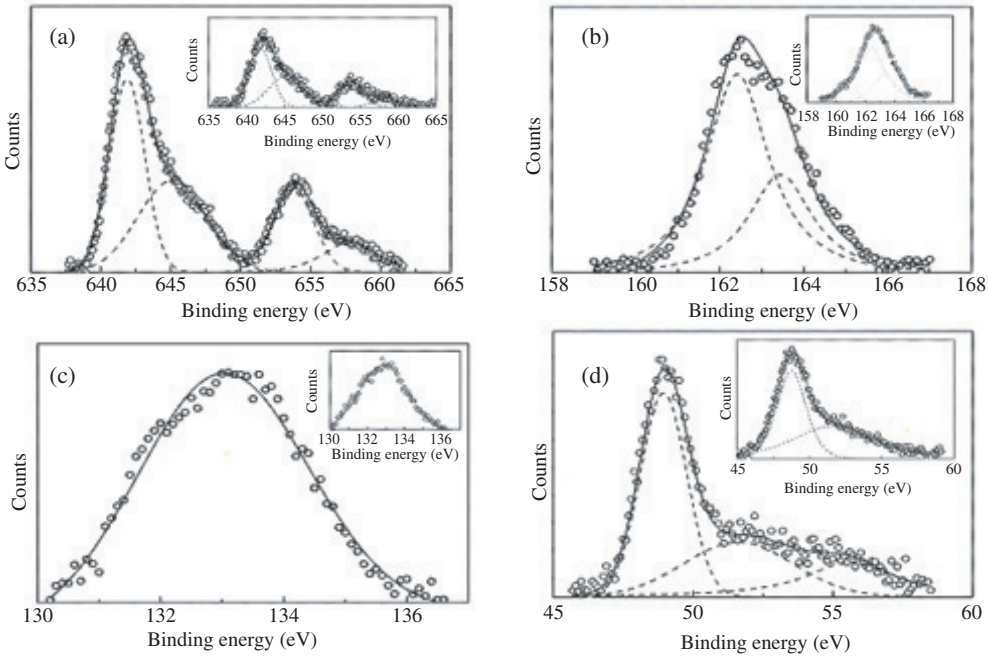

Figure 7. Mn 2p (a), S 2p (b), P 2p (c) Li 1s, and Mn 3p (d) core-level XPS spectra in the nanocomposite thin film and in $MnPS_3$ (inset).

Table 1. Core-level binding energy values in the nanocomposite film, $MnPS_3$ and H_2T_4 salt film referred to the C 1s line (285.0 eV).

Core levels	$MnPS_3$			Nanocomposite film			H_2T_4 salt film		
S 2p	162.4		163.4	162.4	163.4	169.2		169.0	
P 2p		132.9			133.0				
Mn 2p	641.9		653.8	641.9		653.8			
Mn 3p		48.8			48.9				
N 1s				398.7	399.9	401.0	398.9	399.8	401.1
Li 1s					55.6				
O 1s					531.6			531.7	

Table 2. Quantitative XPS data analysis for the nanocomposite and H_2T_4 salt films. S* indicates the sulfur of the cluster $(P_2S_6)^{4-}$ in the lithium exfoliated $MnPS_3$.

Atomic ratio	H_2T_4 salt film	Nanocomposite film
C/N	9.1	9.0
C/O	6.0	6.0
C/S	18.1	18.1
N/S	2.0	2.0
O/S	3.0	3.0
Li/P		0.50
Mn/P		0.75
S*/P		3.0

N 1s core-level XPS spectra are considered to be the most sensitive probe for describing the charge distribution in porphyrins [52]. A comparison of the spectra for the thin films of the nanocomposite and the H_2T_4 salt (figure 5) evidences no remarkable change in the shape or in the binding energy positions. Indeed, both spectra can be described by three Gaussian–Lorentzian bands having area ratios of 1:2:1 and located at 398.7, 399.9 and 401.0 eV for the thin films of the nanocomposite and at 398.9, 399.8 and 401.1 eV for the thin films of the H_2T_4 salt, respectively.

Both these XPS spectra exhibit a strong similarity to those reported by Macquet *et al* for tetrakis(4-pyridyl)porphyrin (H_2TpyP) [53], where three types of nitrogen atoms are present (two aza and two pyrrole type in the macrocycle core, and four pyridine nitrogen atoms on the meso substituent groups). On the basis of the observed area ratio and of the analogy with H_2TpyP, we can attribute the lower-energy peak to the aza nitrogen atoms, the intermediate one to the four *N*-methyl-pyridinium nitrogen atoms, and the higher-energy one to the two pyrrole groups. This assignment is also based on: (i) the higher electronegativity of a pyrrole nitrogen atom with respect to an aza one [53]; (ii) the observed energy separation of the two nitrogen photopeaks characterized by the same area, which agrees well with the value reported in the literature in a free-base porphyrin [54]; and (iii) the good electron-donating ability of a methyl group. Indeed, for the same formal oxidation state, the core-level binding energy increases on increasing the electronegativity of the attached groups. The present data seem to suggest that the nitrogen atoms on the meso substituent groups are not in a cationic state. This observation should imply that the positively charged *N*-methyl-pyridinium groups of H_2T_4 are interacting rather strongly with (i) the negative charge present on the polyanionic layers, or (ii) its tosylate counterion, which is entrapped between the layers.

Experimental evidence supporting H_2T_4 intercalation between $MnPS_3$ layers together with its counterion is provided by the S 2p core-level XPS spectra of the composite thin film (figure 6).

Two features are clearly distinguishable: (i) a poorly resolved but intense spin–orbit doublet with a spin–orbit splitting of about 1.0 eV (see figure 7(b)) at low binding energies; and (ii) a weaker feature at higher binding energies. The observed binding energy value of the doublet peak is in line with the literature data for the same level in neat $MnPS_3$ and in other transition metal thiophosphates [55, 56]. Therefore, the doublet at lower binding energy is safely assigned to the sulfur atom in the $(P_2S_6)^{4-}$ cluster, in which S is in an anionic state. Concerning the weaker structure located at about 169.2 eV, its binding energy value points to a cationic behaviour for S, similar to sulfate [57]. The assignment of this feature to the S atom of the tosylate anion is supported by: (i) the measured area ratios between the 169.2 eV oxygenated S 2p and the O 1s core levels (1:3) and between the N 1s and the 169.2 eV oxygenated S 2p core levels (2:1) reported in table 2; and (ii) the observed binding energy position of the O 1s core levels (table 1), which is typical of a sulfate group [58].

A comparative analysis of Mn 2p, S 2p, P 2p and Mn 3p core-level XPS spectra (figures 7(a)–(d)) evidences only slight differences in the spectral parameters for the composite thin film and the neat $MnPS_3$ (insets of figure 7), emphasizing the absence of a charge transfer mechanism that accompanies the intercalation process. Such a mechanism could occur only from the guest species to the $MnPS_3$ matrix, since $MnPS_3$ can include only donor species which, once intercalated, are in a cationic form [59]. This implies that we should observe reduction of the host matrix and oxidation of the porphyrin. This latter mechanism should not be energetically favoured and is therefore rather unlikely on considering the positive charge on the periphery of this porphyrin and the reduced electron density at the core ($pK_a = 1.4$) [47].

Moreover, Mn 2p and 3p peaks are accompanied by satellite structures at higher binding energies, as is the case in pure $MnPS_3$ and in other transition metal thiophosphates [60]. Such

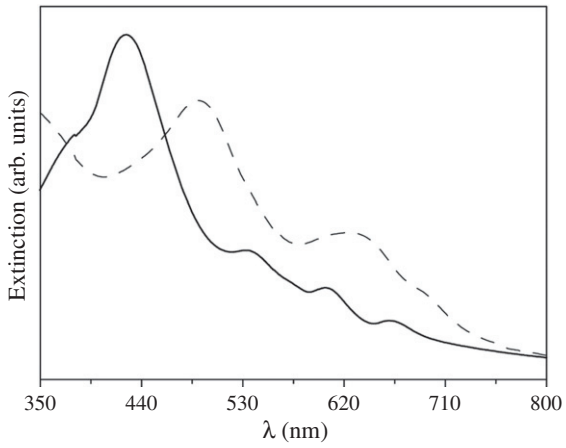

Figure 8. UV–vis absorption spectra of the H_2T_4 salt (solid line) and nanocomposite (dashed line) thin films deposited on glass substrates.

extra features can be identified, in analogy to $NiPS_3$ [60], as *shake-up* lines and suggest that the Mn–S bond is mostly ionic, both in the present layered nanocomposite thin films and in $MnPS_3$ [61, 62]. Moreover, within experimental error, no change is observed in the relative separation between the Mn $2p_{3/2}$ XPS main line and its satellite (locally and non-locally screened XPS final states) on going from the $MnPS_3$ to the nanocomposite film, indicating that no variation in the local cation charge environment occurs, in agreement with what was mentioned above.

In the nanocomposite thin film, the presence of lithium is shown in the Mn 3p core-region XPS spectra (figure 7(d)) at a binding energy (55.6 eV) that is typical of Li^+ [63].

3.3. UV–vis absorption spectroscopy

As reported in the literature, in aqueous solution the porphyrin H_2T_4 exhibits a strong Soret band (B-band) located at 421 nm ($\varepsilon = 2.26 \times 10^5\ M^{-1}\ cm^{-1}$) and a series of four less intense Q-bands at 518, 554, 583 and 638 nm, respectively [47]. As for other meso-aryl substituted porphyrins [64], all these electronic features are strongly dependent of various experimental factors, including structural distortion of the central porphine core or rotation of the meso substituents groups, as well as protonation of the internal nitrogen atoms. Usually, protonation or metal insertion leads to a symmetry change from D_{2h} to D_{2d} or D_{4h}, respectively, with a concomitant reduction of the Q-bands from four to two.

Thin films of the neat H_2T_4 porphyrin salt cast on glass display an intense Soret band at ∼426 nm, accompanied by four Q-bands at ∼536, 560, 609 and 665 nm (figure 8, solid line). These features are consistently shifted in the composite material: the Soret band moves to ∼495 nm with a relevant broadening, while the Q-bands are visible at about 601, 643 and 697 nm (figure 8, dashed line).

3.4. Model for the interaction

Despite its low tendency to self-aggregate in aqueous solutions [65], the tetracationic H_2T_4 porphyrin is able to interact with a variety of polyanionic species. A series of reports in the literature deals with the formation of supramolecular assemblies of this porphyrin and various

analogues with biopolymers such as nucleic acids, synthetic polypeptides and proteins [40], as well as adducts with a variety of charged inorganic materials [37, 66]. In all the cases, the interaction is mainly driven by electrostatic forces between species bearing opposite charges.

In our case, exfoliated $Li_{2x}Mn_{1-x}PS_3$ gives a colloidal suspension, whose stability against flocculation is due to the high negative charge on the constituent layers. When H_2T_4 is added to this system, a rapid interaction occurs, leading to a decrease in the repulsive potential and a consequent collapse of the colloid and the formation of the composite compound. Due to the rapidity of this process, it is reasonable to expect an entrapment of the tosylate counter-anion within the layers. This hypothesis is fully supported by XPS measurements, which show (i) the presence of tosylate anion in the porphyrin composite (also proved by XPS quantitative data: see table 2); and (ii) the presence of lithium ions. All this evidence seems to suggest that charge interactions between the H_2T_4 porphyrin and the anionic inorganic layers have a role in the rapid precipitation of composite films, while in the final product the cationic H_2T_4 porphyrin is charge-balanced by the tosylate anion and this justifies the entrapment of the latter. Therefore, unlike other composite materials [3–9, 11], we can assume that the adduct with the guest is not achieved by ion exchange.

Adsorption of the charged porphyrin on the external surface of the inorganic matrix can be ruled out on the basis of the observed shift of the Soret band ($\Delta\lambda = +69$ nm). Indeed, bathochromic shifts of about 30 nm are reported for external adsorption processes of this porphyrin on laponite [66]. On the other hand, when the porphyrin is intercalated between the inorganic layers, a bathochromic shift of about 60 nm has been observed [66]. Therefore, we can assume that the porphyrin is entrapped between the layers with a mostly parallel arrangement of the porphyrin plane with respect to the exfoliated $Li_{2x}Mn_{1-x}PS_3$ surface. This model is in line with the only slight increase (0.2 Å) of the interlayer spacing measured by the XRD technique, on passing from the lithium intercalate to the final porphyrin composite. Concerning the origin of the observed relevant shift to lower energy of the porphyrin UV/Vis bands, different mechanism could be envisaged: (i) protonation of the central pyrrole nitrogen atoms ($pK_a = 1.4$) [47], with the consequent distortion of the porphine plane; and/or (ii) a rotation of the meso substituent groups towards a flatter conformation. The former mechanism has been mainly proposed, using a combination of resonance Raman and UV/vis spectroscopies, for the interaction of different porphyrins, including H_2T_4, with montmorillonite and fluorohectorite [49]. In these cases, bathochromic shifts up to about 50 nm have been observed, together with broadening of the Soret band and the expected reduction in the number of the Q-bands (even if this point remains unclear, due to severe overlap of the bands). It is interesting to point out also that the interaction of free-base porphyrins with smectite clays usually affords green solids, which is a rough indication of the presence of diacid porphyrins. This behaviour is expected on the basis of the presence of highly active protons on the surface of such inorganic compounds [67–70]. The second mechanism is based on a rotation of the aryl meso groups which determines a flattening of the guest molecule on the charged surface [64, 66]. Semi-empirical PM3 calculations have shown that a 46° twist of the aryl groups with respect to the porphine plane leads to an increase of about 11 kcal mol^{-1} in the energy for the new conformation and explains the observed red-shift of the B-band (60 nm). Rotation of the phenyl groups concomitant to macrocycle saddling distortion have also been invoked recently to describe the observed large red-shifts of the electronic transitions in TPP diacid derivatives, through time-dependent density functional theory [64]. In our case, N 1s core-level XPS spectra indicate the presence of three types of nitrogen atoms in a 1:2:1 relative ratio. Since the corresponding XPS spectra of the diacid species should display only two bands with an area ratio of 1:1, this experimental evidence suggests that H_2T_4 is intercalated between the $MnPS_3$ layers in its unprotonated form. Further support for this hypothesis is given by the

observation of at least three Q-bands in the UV/vis spectra, even if this experimental evidence, once again, should be considered cautiously due to the band overlap in this region.

4. Concluding remarks

The novel hybrid porphyrin/$MnPS_3$ composite has been obtained through an easy solution approach. XPS spectroscopy has proved to be a powerful tool for elucidating the chemical changes at every atomic species involved in the adduct, evidencing the absence of charge transfer processes between the two components. The nature of the interaction leads to a strong flattening of the porphyrin between the layers, which causes one of the most relevant bathochromic shifts of the B-band reported to date for such composite materials. Since the spectral properties of porphyrins can be finely adjusted by introducing groups with different electronic and steric properties and/or by metal coordination, or even by choosing the counter-ions, we expect that such materials can conveniently be exploited in optoelectronic applications. Further investigations of photo-induced conductivity are in progress in our laboratory.

Acknowledgments

The Authors thank Dr Aricò (ITAE-CNR) for technical assistance with XRD measurements and CNR and MIUR for financial support.

References

[1] Clement R 1980 *J. Chem. Soc. Chem. Commun.* 647
[2] Grasso V and Silipigni L 2002 *Riv. Nuovo Cimento* **25** 1
[3] Lacroix P G, Clement R, Nakatami K, Zyss J and Ledoux I 1994 *Science* **263** 658
[4] Gonbeau D, Coradin T and Clement R 1999 *J. Phys. Chem.* B **103** 3545
[5] Coradin T, Clement R, Lacroix P G and Nakatami K 1993 *Chem. Mater.* **8** 2153
[6] Leaustic A, Sour A, Riviere E and Clement R 2001 *C. R. Acad. Sci.* II C **4** 91
[7] Sukpirom N, Oriaki C O and Lerner M M 2000 *Mater. Res. Bull.* **35** 325
[8] Yang D and Frindt R F 2000 *J. Mater. Res.* **15** 2408
[9] Zhang D, Qin J, Yakushi K, Nakasawa Y and Ichimura K 2000 *Mater. Sci. Eng.* A **286** 183
[10] Jeevanandam P and Vasudevan S 1998 *Chem. Mater.* **10** 1276
[11] Lagadic I, Lacroix P G and Clement R 1997 *Chem. Mater.* **9** 2004
[12] Dolphin D (ed) 1978–1979 *The Porphyrins* vol I–VII (New York: Academic)
[13] Darwent J R, Douglas P, Harrison A, Porter G and Richoux M C 1982 *Coord. Chem. Rev.* **44** 83
[14] Richter-Addo G B 2000 *J. Porphyr. Phthalocya.* **4** 354
[15] Chan M K 2000 *J. Porphyr. Phthalocya.* **4** 358
[16] Kim R M, Pillion J E, Burwell D A, Groves J T and Thompson M E 1993 *Inorg. Chem.* **32** 4509
[17] Gibbs E J, Tinoco I J, Maestre M F, Ellinas P A and Pasternack R F 1988 *Biochem. Biophys. Res. Commun.* **157** 350
[18] Pasternack R F, Brigandi R A, Abrams M J, Williams A P and Gibbs E J 1990 *Inorg. Chem.* **29** 4483
[19] Pasternack R F, Bustamante C, Collings P J, Giannetto A and Gibbs E J 1993 *J. Am. Chem. Soc.* **115** 5393
[20] Mukundan N E, Petho G, Dixon D W and Marzilli L G 1995 *Inorg. Chem.* **34** 3677
[21] Pasternack R F, Gurrieri S, Lauceri R and Purrello R 1996 *Inorg. Chim. Acta* **246** 7
[22] Pancoska P, Urbanova M, Bednarova L, Vacek K, Paschenko V Z, Vasiliev S, Malon P and Kral M 1990 *Chem. Phys.* **147** 401
[23] Pasternack R F and Gibbs E J 1993 *J. Inorg. Organomet. Polym.* **3** 77
[24] Nezu T and Ikeda S 1993 *Bull. Chem. Soc. Japan* **66** 25
[25] Purrello R, Scolaro L M, Bellacchio E, Gurrieri S and Romeo A 1998 *Inorg. Chem.* **37** 3647
[26] Purrello R, Raudino A, Scolaro L M, Loisi A, Bellacchio E and Lauceri R 2000 *J. Phys. Chem.* B **104** 10900
[27] Purrello R, Bellacchio E, Gurrieri S, Lauceri R, Raudino A, Scolaro L M and Santoro A M 1998 *J. Phys. Chem.* B **102** 8852

[28] Castriciano M A, Romeo A and Scolaro L M 2002 *J. Porphyr. Phthalocya.* **6** 431
[29] Micali N, Romeo A, Lauceri R, Purrello R, Mallamace F and Scolaro L M 2000 *J. Phys. Chem.* B **104** 9416
[30] Mallamace F, Micali N, Trusso S, Scolaro L M, Romeo A, Terracina A and Pasternack R F 1996 *Phys. Rev. Lett.* **76** 4741
[31] Micali N, Scolaro L M, Romeo A and Mallamace F 1998 *Phys. Rev.* E **57** 5766
[32] Scolaro L M, Romeo A, Mallamace F, Micali N and Purrello R 1998 *Nuovo Cimento* D **20** 2207
[33] Mallamace F, Scolaro L M, Romeo A and Micali N 1999 *Phys. Rev. Lett.* **82** 3480
[34] Mallamace F, Micali N, Romeo A and Scolaro L M 2000 *Curr. Opin. Colloids Interface Sci.* **5** 49
[35] Scolaro L M, Castriciano M A, Romeo A, Mazzaglia A, Mallamace F and Micali N 2002 *Physica* A **304** 158
[36] Ukrainczyk L, Chibwe M, Pinnavaia T J and Boyd S A 1994 *J. Phys. Chem.* **106** 2668
[37] Bizeto M A, De Faria D L A and Constantino V R L 1999 *J. Mater. Sci. Lett.* **18** 643
[38] Nakato T, Iwata Y, Kuroda K, Kaneko M and Kato C 1993 *J. Chem. Soc., Dalton Trans.* **9** 1405
[39] Pinnavaia T J, Chibwe M, Constantino V R L and Yun S K 1995 *Appl. Clay Sci.* **10** 117
[40] Ogawa M and Kurida K 1995 *Chem. Rev.* **95** 399
[41] Bedioui F 1995 *Coord. Chem. Rev.* **144** 39
[42] Bonnet S, Forano C, De Roy A, Besse J P, Maillard P and Momenteau M 1996 *Chem. Mater.* **8** 1962
[43] Pasternack R F and Gibbs E J 1996 *Met. Ions Biol. Syst.* **33** 367
[44] Guliaev A B and Leontis N B 1999 *Biochemistry* **38** 15425
[45] Jeevanandam P and Vasudevan S 1998 *J. Phys. Chem.* B **102** 4753
[46] Silipigni L, Di Marco G, Salvato G and Grasso V 2005 *Appl. Surf. Sci.* **252** 1998
[47] Kalyanasundaram K 1984 *Inorg. Chem.* **23** 2453
[48] Silipigni L, Grasso V, De Luca G, Scolaro L M and Salvato G 2005 *J. Appl. Phys.* **98** 43307
[49] Dias P M, De Faria D L A and Constantino V R L 2000 *J. Incl. Phenom. Macr. Chem.* **38** 251
[50] Briggs D and Riviere J C 1994 *Practical Surface Analysis* 2nd edn, vol 1 *Auger and X-ray Photoelectron Spectroscopy* ed D Briggs and M P Seah (Chichester: Wiley) chapter 3
[51] Niwa Y, Kobayashi H and Tsuchiya T 1974 *J. Chem. Phys.* **60** 799
[52] Karweik D H and Winograd N 1976 *Inorg. Chem.* **15** 2336
[53] Macquet J P, Millard M M and Theophanides T 1978 *J. Am. Chem. Soc.* **100** 4741
[54] Gassman P G, Ghosh A and Almöf J 1992 *J. Am. Chem. Soc.* **114** 9990
[55] Currò G M, Grasso V and Silipigni L 1998 *J. Appl. Phys.* **84** 6693
[56] Calareso C, Currò G M, Grasso V and Silipigni L 2000 *J. Vac. Sci. Technol.* A **18** 306
[57] Moulder J F, Stickle W F, Sobol P E and Bomben K D 1992 *Handbook of X-Ray Photoelectron Spectroscopy* (Eden Prairie, MN: Perkin-Elmer) p 61
[58] Moulder J F, Stickle W F, Sobol P E and Bomben K D 1992 *Handbook of X-Ray Photoelectron Spectroscopy* (Eden Prairie, MN: Perkin-Elmer) p 45
[59] Liang W Y 1986 *Intercalation in Layered Materials* vol 148, ed M S Dresselhaus (New York: Plenum) p 31
[60] Piacentini M, Khumalo F S, Olson C G, Anderegg J W and Lynch D W 1982 *Chem. Phys.* **65** 289
[61] Grasso V, Santangelo S and Piacentini M 1986 *Solid State Ion.* **20** 9
[62] Grasso V, Neri F, Perillo P, Silipigni L and Piacentini M 1991 *Phys. Rev.* B **44** 11060
[63] Moulder J F, Stickle W F, Sobol P E and Bomben K D 1992 *Handbook of X-Ray Photoelectron Spectroscopy* (Eden Prairie, MN: Perkin-Elmer) p 35
[64] Rosa A, Ricciardi G, Baerends E J, Romeo A and Scolaro L M 2003 *J. Phys. Chem.* A **107** 11468
[65] Kano K, Minamizono H, Kitae T and Negi S 1997 *J. Phys. Chem.* A **101** 6118
[66] Chernia Z and Gill D 1999 *Langmuir* **15** 1625
[67] Mortland M M and Raman K V 1968 *Clays Clay Miner.* **16** 393
[68] Mortland M M and Pinnavaia T J 1971 *Nat. Phys. Sci.* **229** 75
[69] Pinnavaia T J and Mortland M M 1971 *J. Phys. Chem.* **75** 3957
[70] Walter R I, Ojadi E C A and Linschitz H 1993 *J. Phys. Chem.* **97** 13308
[71] Scagliotti M, Jouanne M, Balkanski M, Ouvrard G and Benedek G 1987 *Phys. Rev.* B **35** 7097
[72] Polak M 1982 *J. Electron Spectrosc. Relat. Phenom.* **28** 171 and references inside
[73] Veal B W and Paulikas A P 1985 *Phys. Rev.* B **31** 5399
[74] Moulder J F, Stickle W F, Sobol P E and Bomben K D 1992 *Handbook of X-Ray Photoelectron Spectroscopy* (Eden Prairie, MN: Perkin-Elmer) p 23, 29
[75] Woodruff D P and Delchar T A 1994 *Modern Technique of Surface Science* 2nd edn (Cambridge: Cambridge University Press)
[76] Moulder J F, Stickle W F, Sobol P E and Bomben K D 1992 *Handbook of X-Ray Photoelectron Spectroscopy* (Eden Prairie, MN: Perkin-Elmer) p 253